Data-driven Distributionally Adjustable Robust Chance-constrained DG Capacity Assessment

Masoume Mahmoodi, Seyyed Mahdi Noori Rahim Abadi, Ahmad Attarha, Paul Scott, and Lachlan Blackhall

***Abstract*—Moving away from fossil fuels towards renewable sources requires system operators to determine the capacity of distribution systems to safely accommodate green and distributed generation (DG). However, the DG capacity of a distribution system is often underestimated due to either overly conservative electrical demand and DG output uncertainty modelling or neglecting the recourse capability of the available components. To improve the accuracy of DG capacity assessment, this paper proposes a distributionally adjustable robust chance-constrained approach that utilises uncertainty information to reduce the conservativeness of conventional robust approaches. The proposed approach also enables fast-acting devices such as inverters to adjust to the real-time realisation of uncertainty using the adjustable robust counterpart methodology. To achieve a tractable formulation, we first define uncertain chance constraints through distributionally robust conditional value-at-risk (CVaR), which is then reformulated into convex quadratic constraints. We subsequently solve the resulting large-scale, yet convex, model in a distributed fashion using the alternating direction method of multipliers (ADMM). Through numerical simulations, we demonstrate that the proposed approach outperforms the adjustable robust and conventional distributionally robust approaches by up to 15% and 40%, respectively, in terms of total installed DG capacity.**

***Index Terms*—Distributed generation (DG) capacity assessment, distributionally robust optimisation, chance-constrained optimisation, distribution system.**

NOMENCLATURE

A. Parameters

β	Safety factor
$\boldsymbol{\sigma}_t, \boldsymbol{\sigma}_{t'}$	Penalty parameters of augmented Lagrangian in subproblem and master problem of alternating direction method of multipliers (ADMM) algorithms
ϵ	Wasserstein ball radius
γ	Economic viability coefficient
$\hat{\eta}_{j\varphi t}$	Forecasted value of solar efficiency coefficient at node j, phase φ, and time t
$\theta_{i\varphi t}$	Power factor angle at node i, phase φ, and time t
Δt	Length of each time interval
$\underline{\Delta\eta}_t, \overline{\Delta\eta}_t$	Lower and upper bounds on photovoltaic (PV) fluctuation from its forecasted value at time t
$\underline{\Delta p}^d_{j\varphi t}, \overline{\Delta p}^d_{j\varphi t}$	Lower and upper bounds on load fluctuation from its forecasted value at node j, phase φ, and time t
$\boldsymbol{\lambda}_t^{(m)}, \boldsymbol{\lambda}_t'^{(m)}$	Dual variables calculated at iteration m of subproblem and master problem of ADMM algorithms at time t
$\hat{\mathbb{P}}_N$	Nominal probability distribution
$\hat{p}^d_{j\varphi t}$	Forecasted value of real power demand at node j, phase φ, and time t
$\tilde{R}$	Squared voltage sensitivity to real power
$R_p^{(m)}, R_d^{(m)}$	Primal and dual residuals at iteration m of ADMM algorithms
$\underline{U}, \overline{U}$	Lower and upper squared voltage limits
U_0	Squared voltage magnitude of slack node
$\boldsymbol{W}, \boldsymbol{h}$	Constants of uncertainty set
$\tilde{X}$	Squared voltage sensitivity to reactive power

B. Sets

Φ	Set of all phases
Ξ	Set of all random variables
$\mathcal{E}$	Set of all edges
$\mathbb{B}_\epsilon(\hat{\mathbb{P}}_N)$	Wasserstein ball with radius ϵ centred at nominal probability distribution
$\mathbb{R}$	Set of real numbers
$\mathcal{T}$	Set of all time intervals
$\mathcal{U}_d, \mathcal{U}_{pv}$	Demand and PV generation uncertainty sets
$\mathcal{V}$	Set of all nodes
$\mathcal{V}_g$	Set of all nodes and phases with power consumption and/or injection

Manuscript received: January 18, 2023; revised: May 17, 2023; accepted: July 6, 2023. Date of CrossCheck: July 6, 2023. Date of online publication: August 11, 2023.

M. Mahmoodi (corresponding author), S. M. N. R. Abadi, A. Attarha, P. Scott, and L. Blackhall are with the College of Engineering and Computer Science, The Australian National University, Canberra, Australia (e-mail: masoume.mahmoodi@anu.edu.au; mahdi.noori@anu.edu.au; ahmad.attarha@anu.edu.au; Paul.scott@anu.edu.au; Lachlan.blackhall@anu.edu.au).

DOI: 10.35833/MPCE.2023.000029

C. Variables

$\alpha^d_{p,j\varphi t}, \alpha^d_{q,j\varphi t}$	Slopes of real and reactive power adjustments to demand fluctuation at node j, phase φ, and time t
$\alpha^g_{p,j\varphi t}, \alpha^g_{q,j\varphi t}$	Slopes of real and reactive power adjustments to PV generation fluctuation at node j, phase φ, and time t
$\boldsymbol{\xi}$	Vector of all random variables
$\Delta p^d_{j\varphi t}, \Delta\eta_t$	Load and PV efficiency coefficient fluctuations from their forecasted values
$\lambda, \boldsymbol{\mu}_i$	Objective function reformulation related dual variables
$\tilde{\lambda}, \tilde{\boldsymbol{\mu}}_{ij}$	Constraint reformulation related dual variables
$\delta_{\hat{\xi}_i}$	Dirac distribution concentrating unit mass at sample $\hat{\boldsymbol{\xi}}_i$.
$\underline{G}_{j\varphi}, \overline{G}_{j\varphi}$	Lower and upper bounds on PV installation size at node j and phase φ
$G_{j\varphi}$	PV installation capacity at node j and phase φ
$p^{cur0}_{j\varphi t}, q^{g0}_{j\varphi t}$	y-intercepts of real and reactive power adjustment functions at node j, phase φ, and time t
$p^{cur}_{j\varphi t}$	Real power curtailment at node j, phase φ, and time t
$p^d_{j\varphi t}, q^d_{j\varphi t}$	Real and reactive power demands at node j, phase φ, and time t
$p^g_{j\varphi t}, q^g_{j\varphi t}$	Real and reactive power generations at node j, phase φ, and time t
$p_{j\varphi t}, q_{j\varphi t}$	Net real and reactive power consumptions at node j, phase φ, and time t
s_i	Objective function reformulation auxiliary variable
$\tilde{s}_i$	Constraint reformulation auxiliary variable
$U_{i\phi}$	Squared voltage magnitude at node i and phase ϕ
$V_{j\varphi t}$	Complex voltage at node j, phase φ, and time t
$\boldsymbol{x}^a, \boldsymbol{x}^u$	Vectors of adjustable and unadjustable decision variables
$\boldsymbol{y}$	Vector of all decision variables

I. Introduction

THE ever-increasing penetration of distributed generation (DG), particularly solar photovoltaics (PV), can cause technical issues such as reverse power flow and over-voltage in distribution systems [1]. These issues, in turn, limit the amount of DGs that can be installed. Therefore, a DG capacity assessment, which accounts for the time-varying nature of power demand and DG outputs, needs to be performed by the system operators in advance. However, the combination of data uncertainty and the large size of the problem makes DG capacity assessment excessively challenging.

The literature on the topic often simplifies the problem by either ignoring the uncertainty (e.g., [2]-[4]) or opting for over-conservative hosting capacities based on its worst-case realisation (e.g., [5], [6]). Neglecting uncertainty leads to an inaccurate assessment of the distribution system capacity, while the worst-case-oriented approaches have two main shortcomings: ① they judge the hosting capacity based on the worst possible realisation of uncertainty which might rarely happen; ② they neglect DG inverters' capability to provide flexibility. This flexibility is known as active network management (ANM), which can be utilised to open up the distribution system capacity to accommodate more DGs [7].

Recently, with the advances in technology and the Internet of Things, more and more data are being stored [8]. Such historical data can provide valuable information on possible distributions of uncertain parameters, which can be used to make more accurate models. Neglecting such valuable extra information, as with [5], [6], is an inefficient way to handle this problem. The use of information drawn from available data and the ability of smart inverters to provide ANM services are the main gaps in the literature that motivated us to conduct the current study.

In this paper, a more accurate DG hosting capacity study is conducted that not only takes uncertainties into account, but also equips DG inverters with controllers to provide ANM services. To ensure that the study of the hosting capacity is not overly conservative, we use a distributionally robust technique that employs the Wasserstein metric. The proposed approach utilises the available data to build an ambiguity set that includes possible distributions for uncertain parameters; this is because, depending on the amount and quality of the available data, the "true" uncertainty distribution can still be unknown.

In addition, we distinguish between hard and soft constraints in our optimisation modelling, depending on how critical a constraint is. Examples of hard and soft constraints are the physical limits of an inverter and voltage limit constraints, respectively. We then ensure that the hard constraints are satisfied for any realisation within an uncertainty set while allowing the soft constraints to be violated in rare circumstances. The system operator sets the maximum probability of soft constraint violation within the proposed approach. Finally, to ensure that the study of the hosting capacity is scalable to realistically large power systems, we use the alternating direction method of multipliers (ADMM) to break the whole problem into smaller pieces and solve it in a distributed fashion. In the following text, we compare the proposed approach with related work in literature.

II. Related Work

With the increasing global determination to shift towards renewable energy resources, researchers have conducted various DG capacity assessment studies in the literature. References [2], [3], [9], [10] develop deterministic optimisation models, assuming that the electrical demand and PV generation are precisely known ahead of time. This assumption significantly oversimplifies the problem and results in inaccu-

rate DG capacity values.

To incorporate uncertainties into the assessment models, stochastic optimisation (SO) [11] and robust optimisation (RO) [12] have been commonly used in the literature. However, SO often leads to poor out-of-sample performance, while RO leads to overly conservative solutions. To overcome these issues, the third group of approaches, i.e., distributionally robust optimisation (DRO), has recently been introduced [13]. Rather than purely working with the worst-case scenarios as with RO, DRO features an ambiguity set that includes possible distributions for the uncertain parameters. It also improves the out-of-sample performance of SO by immunising the solutions against the worst-case distribution in the ambiguity set, rather than for a single pre-specified one. Furthermore, DRO approaches possess certain advantages over other data-driven approaches such as the randomisation optimisation approach [14], [15]. DRO approaches do not heavily rely on having a vast number of samples [16], which are often unavailable in power system studies. As demonstrated in this paper and other relevant works [17]-[19], DRO approaches are scalable and applicable to large-scale power system planning problems. This scalability makes them a practical choice for addressing uncertainties in power system analysis and planning.

Based on their ambiguity sets, DRO approaches are categorised into moment-based [20] and metric-based [21] approaches. Moment-based approaches only use first- and second-order moments (mean and variance) [22], [23]. An example of a moment-based approach in power system applications is the data-driven DG capacity assessment model developed in [24]. Moment-based approaches forgo other available information besides the first- and second-order moments. In contrast, metric-based DRO approaches such as the Wasserstein metric [13], [25] can leverage additional information present in the available data. Unlike moment-based approaches, metric-based DRO approaches can exploit the full range of data characteristics to enhance accuracy. Thus, to achieve a more precise assessment of the hosting capacity in distribution systems, we choose to employ the Wasserstein metric.

Wasserstein-based DRO has been suggested for power system applications such as unit commitment [26] and optimal power flow [27]-[29]. However, [28] uses Wasserstein-metric in a multi-stage DRO approach. The real-world application of such approaches is limited as they need to solve a large-scale optimisation problem centrally in real time and communicate the corrective actions to fast-acting devices (like inverters) using live communication. To overcome this issue, we propose a new DRO that uses adjustable robust counterpart (ARC) approach [30] to obtain all control actions prior to real time and in the planning stage. Thus, the proposed approach neither counts on live communication nor needs to solve a central large-scale optimisation problem in real time. In addition, unlike [26], [27], and [29] that neglect the impact of ANM schemes, our approach allows fast-acting devices such as inverters to take recourse actions, i.e., to provide reactive power compensation and real power curtailment, in response to uncertainty realisation. Using numerical experiments in Section VII, we show that this increases the net annual PV generation by 50%.

Furthermore, the literature often reduces the horizon of the study of the hosting capacity in favour of the problem size. For instance, [5], [24], and [31] assess the DG capacity of distribution systems for a day, while a study of the DG capacity assessment needs to be carried out for at least a year. Unlike [5], [24], and [31], we assess the hosting capacity using a yearly study. To deal with the resulting large-scale problem, we employ the ADMM [32] and decompose our optimisation problem into smaller subproblems and solve it in a distributed fashion.

To summarise, in this paper, we propose a distributionally robust chance-constrained DG capacity assessment considering ANM. We first model demand and DG output uncertainties within a Wasserstein ambiguity set. Next, we develop an optimisation model that maximises the expected overall DG corresponding to the worst-case distribution in the Wasserstein ambiguity set. We use the constraint-wise robust construction [30] and distributionally robust joint chance-constrained programs to treat hard and soft constraints properly. The constraint-wise robust technique ensures that hard constraints are satisfied for all possible uncertainty realisations, while joint chance-constrained programs allow soft constraints to violate within a pre-determined risk level. We then reformulate the resulting problem into a convex quadratically constrained program, which is decomposed into a master problem and several subproblems to be solved via ADMM. Finally, to further improve the scalability of our proposed approach, we approximate the master problem of ADMM into a separable form that can be solved in parallel. Simulation results show that this approximation reduces the solving time by 94% at the cost of introducing less than 0.2% error.

The main contributions of this paper are described as follows.

1) A Wasserstein-metric-based distributionally adjustable robust joint chance-constrained (WDAR-JCC) optimisation model is proposed to evaluate the DG capacity of distribution systems. Unlike [13], [26], and [33], we utilise the chance-constrained programming to make constraints robust to uncertain parameters' distribution mismatches. Unlike [27], [28], and [34], our modelling enables the decision variables to take recourse actions in response to uncertainties. And unlike the two-stage robust/distributionally robust techniques in [31], [35], our approach makes all decisions in one go prior to real time and thus does not rely on the availability of real-time communication.

2) A reformulation of the WDAR-JCC optimisation model is proposed to allow decomposition using the ADMM algorithm. We show that our reformulation effectively breaks the large centralised problem, which cannot be solved using a common computer, into multiple subproblems that can be solved efficiently using available solvers like CPLEX.

Figure 1 visualises the high-level structure for the rest of this paper. Section III presents the mathematical formulation of the deterministic DG capacity assessment model in three-phase distribution systems. Section IV describes the uncertainty modelling in DG capacity assessment. Section V first

constructs an ambiguity set of possible probability distributions and then introduces the proposed WDAR-JCC optimisation model and its convex reformulation. Section VI provides the solution methodology for the problem. Finally, Sections VII and VIII report numerical simulation results and the main conclusions, respectively.

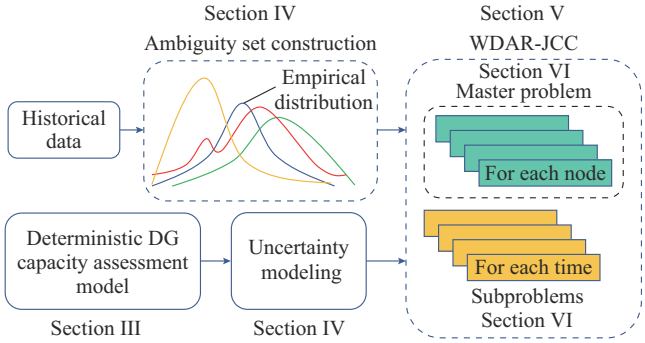

Fig. 1. High-level structure for rest of this paper.

III. Mathematical Formulation

A. Notation

A three-phase distribution system is represented using graph $\mathcal{G}=(\mathcal{V},\mathcal{E})$, where $\mathcal{V}=\{0,1,...,N\}$, and $\mathcal{E}\subseteq\mathcal{V}\times\mathcal{V}$. Node 0 is considered as the slack node, and it is connected to the upstream network. The set of all phases is denoted by $\Phi=\{a,b,c\}$.

Let $p_{j\varphi t}=p^d_{j\varphi t}-p^g_{j\varphi t}$ and $q_{j\varphi t}=q^d_{j\varphi t}-q^g_{j\varphi t}$. Superscripts d and g are used to represent demand and generation, respectively. Without loss of generality, we consider installed PV panels as the only source of generation and model the real power output of the PV inverter using $p^g_{j\varphi t}=\eta_{j\varphi t}G_{j\varphi}-p^{cur}_{j\varphi t}$, where parameter η is the efficiency coefficient, i.e., the ratio of actual generated power to the installed PV capacity. Let us assume constant power factor for the loads, $q^d_{j\varphi t}=p^d_{j\varphi t}\tan\theta_{j\varphi}$, where the power factor angle is constant and given.

In this paper, we use the linear power flow model introduced in [36], as given by:

$$\boldsymbol{U}=\mathbf{1}U_0+\tilde{\boldsymbol{R}}\boldsymbol{p}+\tilde{\boldsymbol{X}}\boldsymbol{q} \tag{1}$$

where $\tilde{\boldsymbol{R}}$ and $\tilde{\boldsymbol{X}}$ are the sensitivity matrices under no-load condition, as given as:

$$\begin{cases}\tilde{R}^{i,\phi}_{j,\varphi}=\dfrac{\partial U_{i\phi}}{\partial p_{j\varphi}}\\ \tilde{X}^{i,\phi}_{j,\varphi}=\dfrac{\partial U_{i\phi}}{\partial q_{j\varphi}}\end{cases} \tag{2}$$

B. Deterministic PV Capacity Assessment Model

In this subsection, we develop a deterministic optimisation model to obtain the PV hosting capacity of the network, which is defined as the total amount of PV that can be installed in a distribution system without the need for expensive reinforcement or hardware upgrade. This model is given as:

$$\max \sum_{(j,\varphi)\in\mathcal{V}_g}\sum_{t\in\mathcal{T}}(\hat{\eta}_{j\varphi t}G_{j\varphi}-p^{cur}_{j\varphi t}) \tag{3}$$

s.t.

$$\underline{U}\le U_0+\sum_{(j,\varphi)\in\mathcal{V}_g}(\tilde{R}^{i,\phi}_{j,\varphi}p_{j\varphi t}+\tilde{X}^{i,\phi}_{j,\varphi}q_{j\varphi t})\le\overline{U} \tag{4}$$

$$p_{j\varphi t}=\hat{p}^d_{j\varphi t}-p^g_{j\varphi t} \tag{5}$$

$$q_{j\varphi t}=q^d_{j\varphi t}-q^g_{j\varphi t} \tag{6}$$

$$q^d_{j\varphi t}=\hat{p}^d_{j\varphi t}\tan\theta_{j\varphi t} \tag{7}$$

$$p^g_{j\varphi t}=\hat{\eta}_{j\varphi t}G_{j\varphi}-p^{cur}_{j\varphi t} \tag{8}$$

$$0\le p^{cur}_{j\varphi t}\le\hat{\eta}_{j\varphi t}G_{j\varphi} \tag{9}$$

$$(\cos\vartheta-\sin\vartheta)p^g_{j\varphi t}+(\cos\vartheta+\sin\vartheta)q^g_{j\varphi t}\le\sqrt{2}\,G_{j\varphi} \tag{10}$$

$$\sum_{t\in\mathcal{T}}p^{cur}_{j\varphi t}\Delta t\le\gamma\sum_{t\in\mathcal{T}}\hat{\eta}_{j\varphi t}G_{j\varphi}\Delta t \tag{11}$$

$$\underline{G}_{j\varphi}\le G_{j\varphi}\le\overline{G}_{j\varphi} \tag{12}$$

Formula (4) represents the voltage constraints $\forall(i,\phi)\in\mathcal{V}$, $t\in\mathcal{T}$ and implies that all the squared voltage magnitudes should be kept within envelope $[\underline{U},\overline{U}]$. Constraint (9) enforces the curtailed power to be positive while not exceeding the PV generated power. Constraints (5)-(9) should be satisfied $\forall(j,\varphi)\in\mathcal{V}_g, t\in\mathcal{T}$. Constraint (10) represents the thermal limit of the inverter, which is approximated with a set of linear inequalities [4]. This constraint needs to be satisfied $\forall(j,\varphi)\in\mathcal{V}_g$, $t\in\mathcal{T}$, $\vartheta\in\Theta:=\{0,\pi/e,2\pi/e,\ldots,(2e-1)\pi/e\}$, where ϑ is a parameter used to approximate the inverter's quadratic thermal constraint with a set of lines [4], and $e\ge2$ is an arbitrary integer number and the accuracy of this approximation increases for higher values of e. Constraint (11) limits the curtailment of PV power output to prevent unrealistically large PV capacities by over-curtailing PV generations and therefore avoid the economic non-viability [6]. Finally, constraint (12) enforces the acceptable range of PV installation capacities. This constraint is included to avoid unrealistically large PV capacities, especially for the nodes in close proximity to the substation, and also allows all the nodes to have the opportunity to install PV units. Both (11) and (12) should be satisfied $\forall(j,\varphi)\in\mathcal{V}_g$. We should point out that our modelling of network safety limits is general and can accommodate various constraints beyond voltage limits. For instance, we can add line congestion margin constraints that specify the maximum real and reactive power that can flow through each line, as demonstrated in [37]. Additionally, voltage unbalance constraints can be incorporated into our optimisation model with slight modifications, as demonstrated in previous studies [38]. However, to avoid over-complicating the model, these constraints are not incorporated into our analysis.

The deterministic model (3)-(12) does not consider the uncertainties of load and PV generation. In the next section, we provide the modelling of these uncertainties.

IV. Uncertainty Modelling

We characterise the uncertainty of loads and PV efficiency coefficients using the following polyhedral uncertainty sets:

$$\mathcal{U}_d := \left\{ p^d_{j\varphi t} \in \mathbb{R} \;\middle|\; p^d_{j\varphi t} = \hat{p}^d_{j\varphi t} + \Delta p^d_{j\varphi t}, \underline{\Delta p}^{\,d}_{j\varphi t} \le \Delta p^d_{j\varphi t} \le \overline{\Delta p}^{\,d}_{j\varphi t} \right\} \quad (13)$$

$$\mathcal{U}_{pv} := \left\{ \eta_t \in \mathbb{R} \;\middle|\; 0 \le \eta_t = \hat{\eta}_t + \Delta\eta_t \le 1, \underline{\Delta\eta}_t \le \Delta\eta_t \le \overline{\Delta\eta}_t \right\} \quad (14)$$

These fluctuations are bounded between given lower and upper bounds.

A. Affine Policies for Inverters

Fast-acting devices such as inverters are able to take recourse actions once uncertainties are realised. We employ affine policies to model control decisions of the inverters. Particularly, we model the real power curtailment and reactive power compensation of each inverter using the following functions:

$$p^{cur}_{j\varphi t}(\Delta\eta_t, \Delta p^d_{j\varphi t}) := p^{cur0}_{j\varphi t} + \alpha^g_{p,j\varphi t}\Delta\eta_t - \alpha^d_{p,j\varphi t}\Delta p^d_{j\varphi t} \quad (15)$$

$$q^g_{j\varphi t}(\Delta\eta_t, \Delta p^d_{j\varphi t}) := q^{g0}_{j\varphi t} - \alpha^g_{q,j\varphi t}\Delta\eta_t + \alpha^d_{q,j\varphi t}\Delta p^d_{j\varphi t} \quad (16)$$

In the above model, the first term shown by $(\cdot)^0$ is the part made based on the forecast and cannot be adjusted in real time. On the contrary, the rest of the functions, i.e., $\alpha^{(\cdot)}_{(\cdot)}\Delta\eta_t$ and $\alpha^{(\cdot)}_{(\cdot)}\Delta p^d_{j\varphi t}$, are adjusted in real time to fine-tune the values of $p^{cur}_{j\varphi t}$ and $q^g_{j\varphi t}$ depending on the true realisations of PV output power and demand. The parameters of these functions are $(\cdot)^0$ and $\alpha^g_p, \alpha^d_p, \alpha^g_q, \alpha^d_q \in \mathbb{R}_+$, which are all obtained during the optimisation, and in live operation, only $\Delta\eta_t$ and $\Delta p^d_{j\varphi t}$ are constantly updated using their local measurements.

It is emphasised that the focus of this paper is a planning problem, where we examine the effect of demand-side response to improve the planning decisions. Therefore, this paper falls into the category of steady-state studies, and its hourly timescale neglects modelling the rapid transient behaviors of inverter controllers. This is because these transients occur on a much faster timescale (in the order of milliseconds) than the changes in uncertainty due to PV generation and electrical demand (in the order of tens of seconds), and therefore can be considered separately [39].

B. PV Capacity Assessment Model Under Uncertainty

To consider load and PV generation uncertainties, we replace the deterministic parameters $\{\hat{\eta}_{j\varphi t}, \hat{p}^d_{j\varphi t}\}$ with the uncertain parameters $\{\eta_{j\varphi t}, p^d_{j\varphi t}\}$ in the model (3)-(12). We also substitute the affine policies (15), (16) in the model (3)-(12) to account for inverters' recourse actions.

For ease of exposition, a random vector $\boldsymbol{\xi} := [\Delta\eta_t, \Delta p^d_{j\varphi t}]$, $\forall (j,\varphi) \in \mathcal{V}_g$, $t \in \mathcal{T}$ is introduced, which collects all PV and load uncertain parameters, and is supported by the uncertainty set $\Xi := \{\mathcal{U}_{pv}, \mathcal{U}_d\} := \{\boldsymbol{\xi} \in \mathbb{R}^k | \boldsymbol{W}\boldsymbol{\xi} \le \boldsymbol{h}\}$, where $\boldsymbol{W} \in \mathbb{R}^{\ell \times k}$ and $\boldsymbol{h} \in \mathbb{R}^\ell$ are the constants obtained from (13) and (14). Also, let vector $\boldsymbol{x} := [G, p^{cur}, q^g] \subseteq \mathbb{R}^n$ collect all the decision variables. Then divide the decision variables $\boldsymbol{x}$ into two categories; adjustable decision variables $\boldsymbol{x}^a := \boldsymbol{x}^a_0 + \boldsymbol{\alpha}\boldsymbol{\xi}$ (in this paper, PV power curtailment and reactive power shown in (15), (16)) and unadjustable decision variables $\boldsymbol{x}^u$ (PV capacity variables in our problem). In other words, we consider $\boldsymbol{x} = [\boldsymbol{x}^a, \boldsymbol{x}^u]^{\mathrm{T}}$.

Note that the proposed approach for uncertainty characterisation is not limited to specific sources of uncertainty. For example, it can be applied similarly to model uncertainties in wind power generation. We can incorporate these uncertainties into our model by utilising a polyhedral uncertainty set similar to what we employed for electrical demand and PV generation. To achieve this, we would extend the definition of our random vector $\boldsymbol{\xi}$ to encompass the errors in wind speed prediction. Subsequently, we would follow analogous modelling and optimisation steps, which will be elaborated upon in the following sections.

Afterwards, we write the uncertain PV capacity assessment model as:

$$\min_{\boldsymbol{x}^u, \boldsymbol{x}^a_0, \boldsymbol{\alpha}} \{\boldsymbol{d}(\boldsymbol{x}^u, \boldsymbol{x}^a_0) + \boldsymbol{c}^{\mathrm{T}}(\boldsymbol{x}^u, \boldsymbol{\alpha})\boldsymbol{\xi}\} \quad (17)$$

s.t.

$$\boldsymbol{A}(\boldsymbol{x}^u, \boldsymbol{\alpha})\boldsymbol{\xi} \le \boldsymbol{b}(\boldsymbol{x}^u, \boldsymbol{x}^a_0) \quad (18)$$

where $\boldsymbol{A}(\cdot)$, $\boldsymbol{b}(\cdot)$, $\boldsymbol{c}(\cdot)$, and $\boldsymbol{d}(\cdot)$ are all linear vector functions in their arguments. Also, the max operator is replaced with min as $\max(a) = \min(-a)$.

The random variable $\boldsymbol{\xi}$ appears in both the objective and constraints of the uncertain problem (17), (18). The uncertain constraints can be categorised as hard or soft constraints, where hard physical constraints need to be satisfied for all uncertainty realisations, whereas soft constraints allow some network limits to be violated if the benefit of such violation for improbable scenarios outweighs the decisions guaranteeing their satisfaction for all the possible realisations. In particular, we consider the curtailment constraint (9), inverter's thermal limit constraint (10), and PV capacity limits (12) as hard constraints, and the rest of the constraints (i.e., voltage constraint (4) and curtailment limit constraint (11)) as soft constraints. To immunise hard constraints against all uncertainty realisations in Ξ, we apply the constraint-wise robust counterpart construction technique [30]. To deal with soft constraints, we formulate them as joint chance constraints where we guarantee their satisfaction with a certain probability level specified by the modeller. Therefore, the immunised form of the uncertain PV capacity assessment model (17), (18) can be written as:

$$\min_{\boldsymbol{x}^u, \boldsymbol{x}^a_0, \boldsymbol{\alpha}} \left\{ \boldsymbol{d}(\boldsymbol{x}^u, \boldsymbol{x}^a_0) + \sup_{\boldsymbol{\xi}} \mathbb{E}^{\mathbb{P}}[\boldsymbol{c}^{\mathrm{T}}(\boldsymbol{x}^u, \boldsymbol{\alpha})\boldsymbol{\xi}] \right\} \quad (19)$$

s.t.

$$\max_{\boldsymbol{\xi} \in \Xi} \{\boldsymbol{E}(\boldsymbol{x}^u, \boldsymbol{\alpha})\boldsymbol{\xi}\} \le \boldsymbol{f}(\boldsymbol{x}^u, \boldsymbol{x}^a_0) \quad (20)$$

$$\mathbb{P}[\boldsymbol{H}(\boldsymbol{x}^u, \boldsymbol{\alpha})\boldsymbol{\xi} \le \boldsymbol{g}(\boldsymbol{x}^u, \boldsymbol{x}^a_0)] \ge 1 - \beta \quad (21)$$

where $\mathbb{E}^{\mathbb{P}}[\cdot]$ shows the expected value of function. $[\boldsymbol{E}^{\mathrm{T}}, \boldsymbol{H}^{\mathrm{T}}]^{\mathrm{T}}$ and $[\boldsymbol{f}^{\mathrm{T}}, \boldsymbol{g}^{\mathrm{T}}]^{\mathrm{T}}$ are all linear vector functions with appropriate dimensions. The model (19)-(21) minimises the worst-case expected objective while satisfying robust hard constraint (20) and also jointly satisfies the chance constraint (21) with a probability of at least $1 - \beta$.

For the sake of notation simplicity, let us collect all the decision variables in vector $\boldsymbol{y} := [\boldsymbol{x}^u, \boldsymbol{x}^a_0, \boldsymbol{\alpha}]$ and update the model (19)-(21) into:

$$\min_{\boldsymbol{y}} \left\{ \boldsymbol{d}(\boldsymbol{y}) + \sup_{\boldsymbol{\xi}} \mathbb{E}^{\mathbb{P}}[\boldsymbol{c}^{\mathrm{T}}(\boldsymbol{y})\boldsymbol{\xi}] \right\} \quad (22)$$

s.t.

$$\max_{\xi \in \Xi} \{\boldsymbol{E}(\boldsymbol{y})\boldsymbol{\xi}\} \leq \boldsymbol{f}(\boldsymbol{y}) \tag{23}$$

$$\mathbb{P}[\boldsymbol{H}(\boldsymbol{y})\boldsymbol{\xi} \leq \boldsymbol{g}(\boldsymbol{y})] \geq 1-\beta \tag{24}$$

where all the vector functions are overloaded to avoid introducing new terms. To solve the problem in (22)-(24), we need to know the probability distribution function $\mathbb{P}$ exactly. However, in most practical situations, the decision maker is not aware of the true underlying distribution of random variables. In the next section, we develop a distributionally robust PV capacity assessment model which immunises the problem in (22)-(24) over a set of possible distributions obtained by the Wasserstein metric.

V. WDAR-JCC Optimisation Model

A. Wasserstein Ambiguity Set

In this sub section, we describe the data-driven distributionally robust technique to solve the problem in (22)-(24). As mentioned earlier, the decision maker typically does not have access to the true distribution of random variables. Instead, a finite set of N observed samples, $\{\hat{\boldsymbol{\xi}}_1, \hat{\boldsymbol{\xi}}_2, \ldots, \hat{\boldsymbol{\xi}}_N\} \subseteq \Xi$, is available at hand. Using these observed samples, we can estimate a distribution $\hat{\mathbb{P}}_N$, known as nominal distribution. A convenient way to construct the nominal distribution is to work with the empirical distribution, which is a discrete uniform distribution of the observed samples:

$$\hat{\mathbb{P}}_N = \frac{1}{N}\sum_{i=1}^{N} \delta_{\hat{\xi}_i} \tag{25}$$

In this paper, we use the Wasserstein metric to construct an ambiguity set as a ball around the nominal distribution (25). Let us first define the Wasserstein metric, which measures the distance between probabilities $\mathbb{P}$ and $\hat{\mathbb{P}}_N$.

Definition (Wasserstein metric): the type-1 Wasserstein metric $d_{\mathrm{w}}(\mathbb{P}, \hat{\mathbb{P}}_N): \Xi \times \Xi \to \mathbb{R}$ is defined as:

$$d_{\mathrm{w}}(\mathbb{P}, \hat{\mathbb{P}}_N) := \inf_{\Pi} \int_{\Xi^2} \left\| \boldsymbol{\xi} - \hat{\boldsymbol{\xi}} \right\| \Pi(\mathrm{d}\boldsymbol{\xi}, \mathrm{d}\hat{\boldsymbol{\xi}}) \tag{26}$$

The Wasserstein metric between $\mathbb{P}$ and $\hat{\mathbb{P}}_N$ can be viewed as the cost of an optimal mass transportation plan Π that minimises the cost of moving from $\mathbb{P}$ to $\hat{\mathbb{P}}_N$, where $\left\| \boldsymbol{\xi} - \hat{\boldsymbol{\xi}} \right\|$ is the cost of moving a unit mass from $\boldsymbol{\xi}$ to $\hat{\boldsymbol{\xi}}$. According to the definition above, the Wasserstein ball with radius ϵ centred at the nominal distribution $\hat{\mathbb{P}}_N$ is given by:

$$\mathbb{B}_{\epsilon}(\hat{\mathbb{P}}_N) := \{\mathbb{P} \in \Xi \,|\, d_{\mathrm{w}}(\mathbb{P}, \hat{\mathbb{P}}_N) \leq \epsilon\} \tag{27}$$

B. Objective Function Reformulation

To evaluate the uncertain terms in the objective function (22), we obtain their worst-case expected value over the Wasserstein ball $\mathbb{B}_{\epsilon}(\hat{\mathbb{P}}_N)$. A tractable convex reformulation of the worst-case expectation of a generic linear function is proposed in [13]. According to this Corollary, the worst-case expectation of $\boldsymbol{c}^{\mathrm{T}}(\boldsymbol{y})\boldsymbol{\xi}$ has a strong dual reformulation as:

$$\begin{cases} \sup\limits_{\mathbb{P} \in \mathbb{B}_{\epsilon}(\hat{\mathbb{P}}_N)} \mathbb{E}^{\mathbb{P}}[\boldsymbol{c}^{\mathrm{T}}(\boldsymbol{y})\boldsymbol{\xi}] = \inf\limits_{\lambda \geq 0, \boldsymbol{s}, \boldsymbol{\mu}} \lambda\epsilon + \dfrac{1}{N}\sum\limits_{i=1}^{N} s_i \\ \text{s.t. } \boldsymbol{c}^{\mathrm{T}}(\boldsymbol{y})\hat{\boldsymbol{\xi}}_i + \boldsymbol{\mu}_i^{\mathrm{T}}(\boldsymbol{h} - \boldsymbol{W}\hat{\boldsymbol{\xi}}_i) \leq s_i \quad \forall i \in \{1, 2, \ldots, N\} \\ \left\| \boldsymbol{W}^{\mathrm{T}}\boldsymbol{\mu}_i - \boldsymbol{c}(\boldsymbol{y}) \right\| \leq \lambda \quad \forall i \in \{1, 2, \ldots, N\} \end{cases} \tag{28}$$

where $\lambda \in \mathbb{R}_+$ and $\boldsymbol{\mu}_i \in \mathbb{R}_+^{\ell}$ are associated with the Wasserstein ball (27) and the uncertainty supports (13) and (14).

C. CVaR-based Reformulation of Distributionally Joint Chance Constraints

As shown in [40], the joint chance constraint (24) is equivalent to the individual chance constraint:

$$\mathbb{P}[Z(\boldsymbol{y}, \boldsymbol{\xi}) \leq 0] \geq 1-\beta \tag{29}$$

$$Z(\boldsymbol{y}, \boldsymbol{\xi}) := \max_{j \in \{1, 2, \ldots, m\}} \{\boldsymbol{H}_j^{\mathrm{T}}(\boldsymbol{y})\boldsymbol{\xi} - g_j(\boldsymbol{y})\} \tag{30}$$

where $\boldsymbol{H}_j^{\mathrm{T}}(\boldsymbol{y})$ denotes the j^{th} row of the matrix $\boldsymbol{H}(\boldsymbol{y})$; and $g_j(\boldsymbol{y})$ is the j^{th} element of the vector $\boldsymbol{g}(\boldsymbol{y})$. Constraint (29) is an individual chance constraint that can be equivalently reformulated as a worst-case conditional value at risk (CVaR) constraint [20], [41], [42].

Remark: for a given measurable loss function L: $\mathbb{R}^k \to \mathbb{R}$, probability distribution $\mathbb{P}$ on $\mathbb{R}^k$, and tolerance $\beta \in (0, 1)$, it is well known that [41]:

$$\mathbb{P}(L(\boldsymbol{\xi}) \leq CVaR_{\beta}(L(\boldsymbol{\xi}))) \geq 1-\beta \tag{31}$$

where $CVaR_{\beta}(L(\boldsymbol{\xi}))$ is the CVaR of the function $L(\boldsymbol{\xi})$ at the confidence level β. Thus, $CVaR_{\beta}(L(\boldsymbol{\xi})) \leq 0$ is sufficient to imply that $\mathbb{P}(L(\boldsymbol{\xi}) \leq 0) \geq 1-\beta$.

Using the above remark, the chance constraint (29) can be reformulated as:

$$CVaR_{\beta}(Z(\boldsymbol{y}, \boldsymbol{\xi})) \leq 0 \tag{32}$$

We then use the CVaR definition introduced in [41]:

$$CVaR_{\beta}(Z(\boldsymbol{y}, \boldsymbol{\xi})) := \inf_{\varrho \in \mathbb{R}} \left\{ \varrho + \frac{1}{\beta}\mathbb{E}_{\mathbb{P}}[(Z(\boldsymbol{y}, \boldsymbol{\xi}) - \varrho)^+] \right\} \tag{33}$$

where $(\cdot)^+ = \max(\cdot, 0)$.

We then require the CVaR constraint (33) to hold for a family of distributions defined directly from observed samples via the Wasserstein metric. Therefore, the worst-case CVaR constraint (32) is re-expressed as:

$$\sup_{\mathbb{P} \in \mathbb{B}_{\epsilon}(\hat{\mathbb{P}}_N)} \inf_{\varrho \in \mathbb{R}} \left\{ \varrho + \frac{1}{\beta}\mathbb{E}_{\mathbb{P}}[(Z(\boldsymbol{y}, \boldsymbol{\xi}) - \varrho)^+] \right\} \leq 0 \tag{34}$$

With a similar approach to (28), we can now reformulate (34) as a finite-dimensional convex program given by (35) (see the Proposition 3.1 in [40] for details of this reformulation).

$$\begin{cases} \tilde{\lambda}\epsilon + \dfrac{1}{N}\sum\limits_{i=1}^{N} \tilde{s}_i \leq \varrho\beta \\ \text{s.t. } -g_j(\boldsymbol{y}) + \varrho + (\boldsymbol{H}_j^{\mathrm{T}}(\boldsymbol{y}) - \boldsymbol{W}^{\mathrm{T}}\tilde{\boldsymbol{\mu}}_{ij})^{\mathrm{T}}\hat{\boldsymbol{\xi}}_i + \tilde{\boldsymbol{\mu}}_{ij}^{\mathrm{T}}h \leq \tilde{s}_i \quad \forall i \in \{1, 2, \ldots, N\} \\ \left\| \boldsymbol{W}^{\mathrm{T}}\tilde{\boldsymbol{\mu}}_{ij} - \boldsymbol{H}_j^{\mathrm{T}}(\boldsymbol{y}) \right\| \leq \tilde{\lambda} \\ \tilde{\lambda} \geq 0, \varrho \in \mathbb{R}, \tilde{\boldsymbol{\mu}}_{ij} \geq 0, \tilde{s}_i \geq 0 \end{cases} \tag{35}$$

Note that function $Z(\boldsymbol{y}, \boldsymbol{\xi})$ is substituted with (30) before

applying the reformulation.

D. Robust Constraints

As mentioned earlier, we apply the constraint-wise robust counterpart approach to deal with hard constraints. We use the max protection function (23), to robustify the constraints against the worst uncertainty realisation within Ξ. We then utilise the duality approach described in [43] to replace (23) with a finite set of linear inequality constraints:

$$\exists \boldsymbol{\rho}: \boldsymbol{h}^{\mathrm{T}}\boldsymbol{\rho} \le \boldsymbol{f}(\boldsymbol{y}), \boldsymbol{W}^{\mathrm{T}}\boldsymbol{\rho} \ge \boldsymbol{E}(\boldsymbol{y}) \tag{36}$$

where $\boldsymbol{\rho}$ is the vector of dual variables associated with the bounding constraints in the uncertainty set Ξ.

In summary, we model the Wasserstein distributionally adjustable robust chance-constrained PV capacity assessment model using (37)-(40), which is a convex conic program and solvable using commercial solvers such as CPLEX.

$$\inf_{\boldsymbol{y},\lambda,s,\boldsymbol{\mu},\tilde{\lambda},s,\tilde{\boldsymbol{\mu}}} \left\{ d(\boldsymbol{y}) + \lambda\epsilon + \frac{1}{N}\sum_{i=1}^{N} s_i \right\} \tag{37}$$

s.t.

$$\boldsymbol{c}^{\mathrm{T}}(\boldsymbol{y})\hat{\boldsymbol{\xi}}_i + \boldsymbol{\mu}_i^{\mathrm{T}}(\boldsymbol{h} - \boldsymbol{W}\hat{\boldsymbol{\xi}}_i) \le s_i \tag{38}$$

$$\left\| \boldsymbol{W}^{\mathrm{T}}\boldsymbol{\mu}_i - \boldsymbol{c}^{\mathrm{T}}(\boldsymbol{y}) \right\| \le \lambda \tag{39}$$

$$(35),\ (36) \tag{40}$$

It is worth noting that the OPF model (37)-(40) allows for extensions incorporating additional technologies such as distributed generators beyond PV or voltage control devices like OLTCs. However, to maintain simplicity and focus, we have deferred exploring these extensions and their impact on the final hosting capacity value to future research endeavours.

Since PV capacity assessment is a planning study and depending on the period of the study and temporal resolution of the demand and PV generation samples, it typically has a very large scale. Therefore, the WDAR-JCC optimisation model (37)-(40), despite being convex, is a challenging large-scale optimisation problem that is not easily solvable using the centralised approaches. Note that in addition to the study period and resolution of data, the number of constraints of this problem increases with the number of samples, leading to high dimensionality. In the next section, we present a novel formulation based on ADMM algorithm as an alternative solution methodology to deal with such large-scale optimisation problems.

VI. Solution Methodology

In this section, we present the decomposition methodology using the ADMM algorithm. The ADMM algorithm can decompose the problem into many user-defined subproblems which negotiate over their common variables. In our case, we exploit the specific structural properties of the multi-time PV capacity assessment problem, where we decompose the problem over time. By doing so, we end up with many smaller subproblems where each subproblem is defined over a time interval, and therefore, the subproblems are solved independently of each other. The time-coupled variables are then negotiated between the subproblems and the master problem, which contains all the constraints that are coupled between all time intervals such as curtailment constraint (11) to obtain a feasible solution.

We will further benefit from the specific structural properties of the master problem and propose a separable formulation which allows decomposing the master problem to several smaller subproblems, and therefore, solve them in a parallel fashion. By doing so, we significantly break down the computation time of the master problem and hence the PV capacity assessment problem.

An overview of our decomposition methodology is shown in Fig. 2. At each iteration of the ADMM algorithm, we first solve the subproblems and the decomposed form of the master problem. Then, the ADMM dual variables are updated and the primal and dual residuals are calculated. At last, we check the stopping criteria and if they are satisfied, the ADMM algorithm converges; otherwise, it will continue to the next iteration.

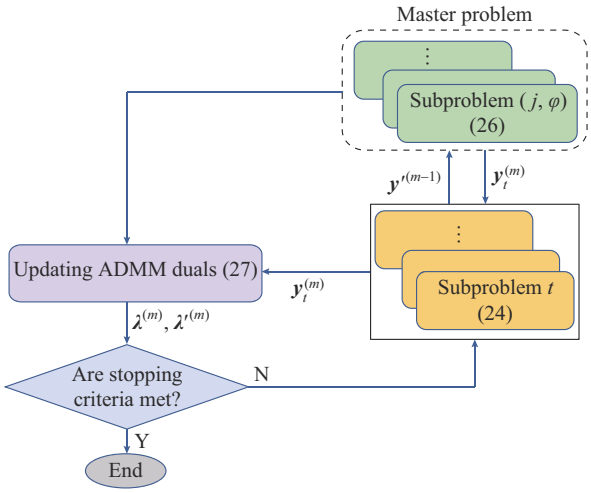

Fig. 2. Overview of decomposition methodology.

In the following, the details of each block of our algorithm are presented.

A. Subproblem Model

Let us consider the general form of the uncertain PV capacity assessment model (22)-(24) and define $\boldsymbol{y}_t := [\boldsymbol{x}_t^u, \boldsymbol{x}_{0_t}^a, \boldsymbol{\alpha}_t]$ which denotes the decision variables of the subproblem corresponding to the time interval t, and $\boldsymbol{y}' := [\boldsymbol{x}^{u\prime}, \boldsymbol{x}_0^{a\prime}, \boldsymbol{\alpha}']$ as the decision variables of the master problem which contains the decision variables for all time intervals. Then, each subproblem is formulated as:

$$\boldsymbol{y}_t^{(m)} := \arg\min_{\boldsymbol{y}_t} \left(\boldsymbol{d}(\boldsymbol{y}_t) + \boldsymbol{\lambda}_t^{(m-1)} \left| \boldsymbol{y}_t - \boldsymbol{y}_t^{\prime(m-1)} \right| + \frac{\boldsymbol{\sigma}_t}{2} \left| \boldsymbol{y}_t - \boldsymbol{y}_t^{\prime(m-1)} \right|^2 \right) \tag{41}$$

s.t.

$$\max_{\boldsymbol{\xi}_t \in \Xi} \{ \boldsymbol{E}(\boldsymbol{y}_t)\boldsymbol{\xi}_t \} \le \boldsymbol{f}(\boldsymbol{y}_t) \tag{42}$$

$$\mathbb{P}[\boldsymbol{H}^v(\boldsymbol{y}_t)\boldsymbol{\xi}_t \le \boldsymbol{g}^v(\boldsymbol{y}_t)] \ge 1 - \beta_t^v \tag{43}$$

where $\boldsymbol{y}_t^{\prime(m-1)} := [\boldsymbol{x}^{u\prime(m-1)}, \boldsymbol{x}_{0_t}^{a\prime(m-1)}, \boldsymbol{\alpha}_{t'}^{(m-1)}]$ denotes the decision

variables of the master problem corresponding to the time interval t, which is obtained in the iteration $m-1$ and therefore is known. Note that $\boldsymbol{x}^{u\prime(m-1)}$ does not have subscript t as it shows the PV capacities $G'_{j\varphi}$.

To solve each subproblem (41) - (43), robust constraints (42) and distributionally robust joint chance constraints (43) are reformulated similar to (36) and (35).

B. Master Problem Model

The master problem is defined over the constraints which couple all the time intervals, and the worst-case expectation of the objective, the second term in (22), which is the summation of PV generations over all time intervals, as given by:

$$\boldsymbol{y}'^{(m)}:=\underset{\boldsymbol{y}'}{\operatorname{argmin}}\left\{\sup_{\xi}\ \mathbb{E}^{\mathbb{P}}[\boldsymbol{c}^{\mathrm{T}}(\boldsymbol{y}')\boldsymbol{\xi}]+\boldsymbol{\lambda}'^{(m-1)}\left|\boldsymbol{y}'-\boldsymbol{y}^{(m)}\right|+\frac{\boldsymbol{\sigma}'}{2}\left|\boldsymbol{y}'-\boldsymbol{y}^{(m)}\right|^2\right\} \tag{44}$$

s.t.

$$\mathbb{P}[\boldsymbol{H}^c(\boldsymbol{y}')\boldsymbol{\xi}\le\boldsymbol{g}^c(\boldsymbol{y}')]\ge 1-\beta^c \tag{45}$$

where vector $\boldsymbol{y}^{(m)}$ collects the decision variables of all subproblems which are obtained at the iteration m; vector $\boldsymbol{\lambda}'^{(m-1)}$ denotes the dual variables of the master problem that are obtained at the iteration $m-1$; vector $\boldsymbol{\sigma}'$ is the constant penalty parameter; the superscript c in the risk level β^c shows that these joint chance constraints correspond to the uncertain form of the curtailment constraint (9) which limits the amount of allowable PV output curtailment to preserve the economic viability; and vector functions $\boldsymbol{H}^c$ and $\boldsymbol{g}^c$ are used to show the portion of chance constraints that correspond to the curtailment constraints.

Constraint (45) shows the joint satisfaction of the curtailment constraint for all prosumers. Fortunately, these constraints are independent, where constraint (45) represents the general form of the constraint (11) which needs to be satisfied for each customer and therefore customers can be treated independently, and therefore we can further decompose them for each prosumer. On the other hand, the term $\boldsymbol{c}^{\mathrm{T}}(\boldsymbol{y}')\boldsymbol{\xi}$ in the objective (44), which is derived from (3) in our PV capacity assessment problem, is separable (for each node). Here, we propose to approximate the model (44), (45) with a set of optimisation models where each is defined for a prosumer, i.e., $\forall(j,\varphi)\in\mathcal{V}_g$:

$$\boldsymbol{y}'^{(m)}_{j\varphi}:=\underset{\boldsymbol{y}'_{j\varphi}}{\arg\min}\left\{\sup_{\xi_{j\varphi}}\mathbb{E}^{\mathbb{P}}[\boldsymbol{c}^{\mathrm{T}}(\boldsymbol{y}'_{j\varphi})\boldsymbol{\xi}_{j\varphi}]+\boldsymbol{\lambda}'^{(m-1)}_{j\varphi}\left|\boldsymbol{y}'_{j\varphi}-\boldsymbol{y}^{(m)}_{j\varphi}\right|+\frac{\boldsymbol{\sigma}'_{j\varphi}}{2}\left|\boldsymbol{y}'_{j\varphi}-\boldsymbol{y}^{(m)}_{j\varphi}\right|^2\right\} \tag{46}$$

s.t.

$$\mathbb{P}[\boldsymbol{H}^c(\boldsymbol{y}'_{j\varphi})\boldsymbol{\xi}_{j\varphi}\le\boldsymbol{g}^c(\boldsymbol{y}'_{j\varphi})]\ge 1-\beta^c_{j\varphi} \tag{47}$$

The advantage of this formulation is that they can be solved in parallel, and therefore, speed up the solving time.

C. Updating Dual Variables

After solving the subproblems (41) - (43) and the decomposed form of the master problem (46), (47), the dual variables are updated using:

$$\boldsymbol{\lambda}_t^{(m)}=\boldsymbol{\lambda}_t^{(m-1)}+\boldsymbol{\sigma}_t(\boldsymbol{y}_t^{(m)}-\boldsymbol{y}_t'^{(m)})\quad\forall t\in\mathcal{T} \tag{48}$$

$$\boldsymbol{\lambda}'^{(m)}_{j\varphi}=\boldsymbol{\lambda}'^{(m-1)}_{j\varphi}+\boldsymbol{\sigma}'_{j\varphi}(\boldsymbol{y}'^{(m)}_{j\varphi}-\boldsymbol{y}^{(m)}_{j\varphi})\quad\forall j\varphi\in\mathcal{V}_g \tag{49}$$

D. Stopping Criteria and Convergence of Algorithm

We define the stopping criteria using primal and dual residuals $R_p^{(m)}$ and $R_d^{(m)}$ as:

$$\begin{cases}R_p^{(m)}:=\boldsymbol{y}'^{(m)}-\boldsymbol{y}^{(m)}\\ R_d^{(m)}:=\boldsymbol{\lambda}'^{(m)}-\boldsymbol{\lambda}^{(m)}\end{cases} \tag{50}$$

In this paper, we consider the problem to have converged when the 2-norms of the primal and dual residuals are both smaller than 10^{-4}.

Note that our final model, i.e., (41) - (43), (46) - (50), is a convex quadratic model for which the convergence of the ADMM algorithm is guaranteed [43].

VII. Numerical Results and Discussion

We examine the performance of the proposed approach on a modified unbalanced IEEE 37-node distribution system as well as IEEE European low-voltage 906-node network to demonstrate the scalability of the proposed approach. We use [0.95, 1.05]p.u. as the acceptable voltage envelope while the voltage of the slack node is kept constant at 1 p.u.. In the following text, we first briefly introduce our simulation data and then demonstrate the results for each test system. Specifically, we investigate the PV capacity assessment results using the WDAR-JCC optimisation model. We also use Monte Carlo simulations to compare the out-of-sample performance of the proposed approach with other state-of-the-art approaches.

A. Simulation Data

We use the 32-year historical hourly PV efficiency coefficient data from [44], as shown in Fig. 3.

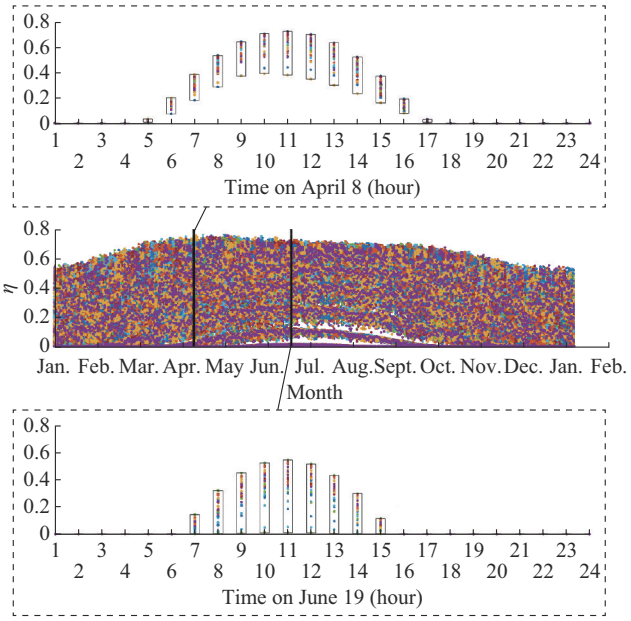

Fig. 3. Historical hourly PV efficiency coefficient data for 32 years.

The data are zoomed in for two days, i. e., April 8 and June 19 (as an example of a rainy day), to provide a better picture of the data. At each hour, we have 32 samples of PV efficiency coefficients (one per year), by which we form a box containing all the historical values. The blue line is the average of the observed values at each hour and will be used as the forecasted values. For electrical demand, we use the data from [45], which is for one year and has a 5 min resolution.

We first convert them to hourly data using averaging technique, and then, without loss of generality, for each hour, we randomly generate 32 values (to match the PV data) such that they deviate from the given value by 10% while following a Gaussian distribution.

We split the available samples into training and test sets. Eighty percent of the data are used for training and the remaining 20% are used for evaluating the out-of-sample performance of the proposed approach.

B. Results for IEEE 37-node Distribution System

1) PV Capacity Assessment Results Using Proposed Approach

In this part, we investigate the performance of the proposed model to obtain the total PV installation capacities and net PV generation for the candidate nodes (six nodes) in the test system. The study period is considered to be one year with the hourly resolutions for PV and demand data. Since the PV efficiency coefficient typically takes on non-zero values during the daytime, we only consider 9 hours (from 08: 00 to 16: 00) per day for analysis. As mentioned earlier, the considered ANM schemes include inverters' reactive power compensation and real power curtailment.

To investigate the sensitivity of the results to different risk levels of the chance constraints, i.e., β_t^v in (41)-(43) and $\beta_{j\varphi}^c$ in (46), (47), we repeat our experiments for three different values $\beta_t^v=\beta_{j\varphi}^c=\beta\in\{0.01,0.05,0.1\}$, which implies that all voltage constraints and curtailment chance constraints are satisfied with confidences of 99%, 95%, and 90%, respectively. Other model parameters are summarised in Table I. For these experiments, we fix the Wasserstein radius at $\epsilon=0.01$. Later in this subsection, we will investigate the sensitivity of the results to the Wasserstein metric.

TABLE I
MODEL PARAMETERS

Parameter	Value
γ	0.1
e	8
θ	$\cos^{-1}(1)$
σ	0.5
$[\underline{G}_{j,\varphi}, \overline{G}_{j,\varphi}]$	$[P_{j,\varphi}^{nom}, 10P_{j,\varphi}^{nom}]$

We use the above-mentioned parameters to solve (41)-(43), (46)-(49). After ADMM converges, the decision variables G, p^{cur0}, q^{g0}, $\boldsymbol{\alpha}_p^g$, $\boldsymbol{\alpha}_p^d$, $\boldsymbol{\alpha}_q^g$, and $\boldsymbol{\alpha}_q^d$ are obtained. The total PV installation capacities for different risk levels are shown in Fig. 4(a). As can be observed, by allowing more violations (larger β), we can install more PVs in the system.

We also obtain the out-of-sample performance for the yearly net PV generation using the test samples whose boxplots are shown in Fig. 4(b). To provide a better intuition, the average PV annual generation is shown in Table II. As can be observed, increasing the risk level or in other words allowing more constraint violations leads to higher net PV generation in the system.

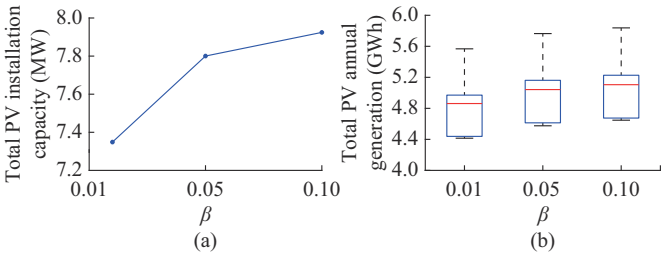

Fig. 4. Out-of-sample performance of proposed approach when risk level $\beta=\beta_t^v=\beta_{j\varphi}^c$ varies while Wasserstein radius is fixed ($\epsilon=0.01$). (a) Total PV installation capacities. (b) Total PV annual generation.

TABLE II
AVERAGE PV ANNUAL GENERATION FOR DIFFERENT RISK LEVELS

β	Average PV annual generation (GWh)
0.01	4.90
0.05	5.09
0.10	5.13

We then fix the risk levels $\beta_t^v=\beta_{j\varphi}^c=0.1$ and vary the Wasserstein metric ϵ to observe the sensitivity of the results to the radius of the Wasserstein ball. We try three different values $\{0.001, 0.01, 0.1\}$ and represent the results in Fig. 5(a) for the total PV installation capacities and Fig. 5(b) as the out-of-sample total PV annual generation. It is observed that with the increase in the Wasserstein radius, the results become more conservative. For instance, the total PV installation capacity is 8.32 MW when $\epsilon=0.001$, while it is 7.35 MW when $\epsilon=0.1$, which shows the decrease of 11.66%. The average PV annual generations for different ϵ are summarised in Table III. As can be observed, the average PV annual generation decreases when the ϵ increases. For instance, we observe the decrease of 8.9% when ϵ changes from 0.001 to 0.1. Therefore, in cases where we have access to more samples, we can construct smaller ambiguity sets, which in turn result in less conservative results.

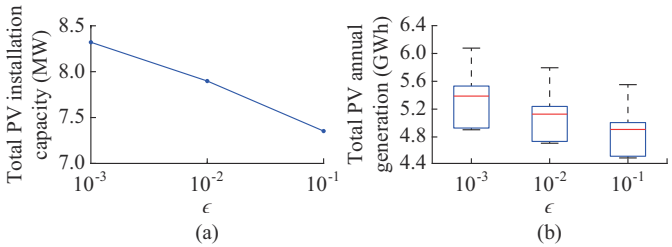

Fig. 5. Out-of-sample performance of proposed approach when Wasserstein radius ϵ varies while risk level is fixed ($\beta=0.1$). (a) Total PV installation capacities. (b) Total PV annual generation.

TABLE III
AVERAGE PV ANNUAL GENERATION FOR DIFFERENT WASSERSTEIN RADIUSES

ϵ	Average PV annual generation (MW)
0.001	5.39
0.010	5.13
0.100	4.90

2) Computational Impact of Proposed Distributed Solution Methodology

In this part, we investigate how the proposed separable formulation (46), (47) impacts the optimisation problem characteristics such as the number of constraints (NoC), number of variables (NoV), number of non-zeros (NNZ), and the solving time. These values for the distributed models before and after applying our approximation, i.e., solving (41)-(45), (48)-(50) compared with solving (41)-(43), (46)-(50), are summarised in Table IV for the under-study network. Since the proposed formulation breaks down the problem per each node and there are six candidate nodes in the network, the number of variables, constraints and non-zeros are decreased by a factor of 6. Therefore, in larger networks with more candidate nodes, this formulation can be even more effective. We observe that the proposed separable formulation significantly breaks down the computational time, from around 4600 s to 280 s, which is in fact around 94% decrease in the solving time. In return, it only introduces less than 0.2% error in the calculated decision variables.

TABLE IV
COMPARISON BETWEEN CENTRAL AND TWO DISTRIBUTED SOLUTION METHODOLOGIES IN TERMS OF NOV, NOC, NNZ, AND SOLVING TIME

Solution methodology	NoV	NoC	NNZ	Solving time (s)
Central (37)-(40)	Not solvable			
Distributed (41)-(45), (48)-(50)	4.1×10^6	331	6.49×10^6	4600
Proposed distributed (41)-(43), (46)-(50)	6.8×10^5	56	1.08×10^6	280

3) Comparison with Other State-of-the-art Approaches

In this part, we use Monte Carlo simulations to compare the results of the proposed approach with the other state-of-the-art approaches. In particular, we compare the propsoed approach with the adjustable robust PV capacity assessment model to evaluate the effectiveness of using distribution information of the uncertain parameters. We also investigate the impact of inverters' recourse actions by comparing the proposed approach with the conventional distributionally robust model, where the capability of inverters to take recourse actions is not considered. By doing so, we will also demonstrate the significance of modelling ANM schemes when investigating the hosting capacity of a distribution system.

Similar to the previous subsection, we first fix the Wasserstein metric to $\epsilon=0.01$ and vary the risk level as $\beta\in\{0.01, 0.05, 0.1\}$. Figure 6(a) and (b) shows the total PV installation capacities and out-of-sample total PV annual generation for the proposed model compared with the corresponding values obtained using the adjustable robust approach. As can be observed, the results of adjustable robust approach is more conservative than the proposed approach. For a fixed Wasserstein metric, if we allow for higher risk levels, i.e., larger β, we can obtain higher PV installation capacities and total PV annual generation. For instance, allowing 10% risk level, the total PV annual generation increases by 11.5% on average (5.13 GWh compared with adjustable robust case which is 4.6 GWh), and also the total PV installation capacity increases from 7.23 MW to 7.9 MW (9.3% increase). We then fix the risk level at $\beta=0.1$ and vary the Wasserstein metric. Figure 6(c) and (d) compares the results for different values of ϵ. The larger Wasserstein metric leads to larger uncertainty set which in turn results in more conservative results, and therefore gets closer to the robust case. For instance, using metric $\epsilon=0.1$ the net annual PV generation (on average) is only 4.6% more than robust case whereas if we can choose smaller metrics like $\epsilon=0.001$, this percentage increases to 15.4%.

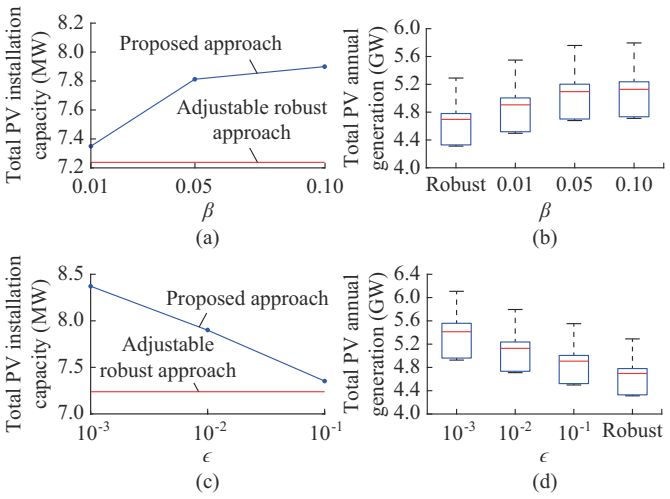

Fig. 6. Comparison between out-of-sample performance of proposed approach and adjustable robust approach. (a) Total PV installation capacities when risk level β varies ($\epsilon=0.01$ is fixed). (b) Total PV annual generation when risk level β varies ($\epsilon=0.01$ is fixed). (c) Total PV installation capacities when ϵ varies while $\beta=0.1$ is fixed. (d) Total PV annual generation when ϵ varies while $\beta=0.1$ is fixed.

We have conducted additional experiments to evaluate the out-of-sample performance of the proposed approach compared with the conventional distributionally robust approach. In the conventional approach, the capability of inverters to take recourse actions is not considered when determining total PV installation capacities and total PV annual generation. Figure 7 illustrates the findings, indicating that incorporating inverters' recourse capabilities lead to a significant improvement. Specifically, we observed an increase of up to 50% in total PV installation capacity and a 40% increase in net PV annual generation. These results unequivocally demonstrate the importance of integrating an ANM scheme in hosting capacity analysis to avoid underestimating the hosting capacity.

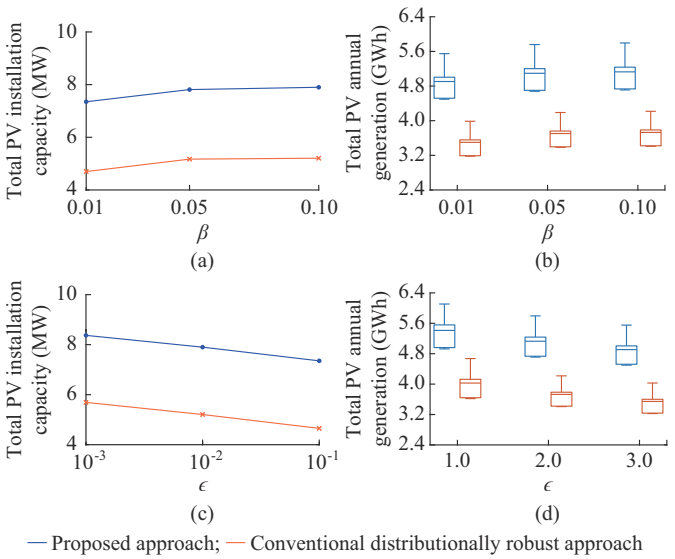

Fig. 7. Comparison between out-of-sample performance of proposed approach and conventional distributionally robust approach (capability of inverters to take recourse actions is not considered). (a) Total PV installation capacities when β varies while $\epsilon = 0.01$ is fixed. (b) Total PV annual generation when β varies while $\epsilon = 0.01$ is fixed. (c) Total PV installation capacities when ϵ varies while $\beta = 0.1$ is fixed. (d) Total PV annual generation when ϵ varies while $\beta = 0.1$ is fixed.

C. Results for IEEE European Low-voltage 906-node Network

To demonstrate the scalability and practical applicability of the proposed approach, we have conducted experiments on the IEEE European low-voltage 906-node network. By utilising the same model parameters outlined in Table I, we maintain consistency and avoid redundancy. Fixed values β and ϵ are set to be 0.1 and 0.01, respectively, and the total PV installation capacities and median PV annual generation are calculated. Additionally, similar calculations are performed for alternative approaches such as the adjustable robust model that incorporates distribution information of uncertain parameters, and the conventional distributionally robust model, which assesses the impact of inverters' recourse actions.

The summary of simulation results in IEEE European low-voltage 906-node network is presented in Table V, affirming the superior performance of the proposed approach compared with the existing approaches. Notably, the proposed approach surpasses the adjustable robust approach by achieving a 12% improvement in total PV installation capacity. Similarly, it outperforms the conventional distributionally robust approach by 47%. Furthermore, in terms of total PV annual generation, the proposed approach exhibits a 14.5% and 37.6% advantage over these approaches, respectively.

To further assess the scalability of the proposed approach, we compared the computing time with that of alternative approaches. The results of these simulations on a MacBook Pro M1 with 8 GB of memory using the CPLEX solver are presented in Table VI. As can be observed, the proposed approach demonstrates comparable computational efficiency to both the adjustable robust and conventional distributionally robust approaches, while simultaneously yielding increased hosting capacity for the network.

TABLE V
SUMMARY OF SIMULATION RESULTS IN IEEE EUROPEAN LOW-VOLTAGE 906-NODE NETWORK

Approach	Total PV installation capacity (kW)	Total PV annual generation (MWh)
Proposed	793	245
Adjustable robust	707	214
Distributionally robust	540	178

TABLE VI
COMPUTING TIME IN IEEE EUROPEAN LOW-VOLTAGE 906-NODE NETWORK FOR DIFFERENT APPROACHES

Approach	Computing time (s)
Proposed	820
Adjustable robust	630
Distributionally robust	780

Overall, these results validate the efficacy of the proposed approach in terms of scalability, practicality, and its ability to outperform alternative approaches, thereby highlighting its potential in real-world applications.

VIII. CONCLUSION

This paper proposes a data-driven approach based on distributionally robust chance-constrained programs to determine the capacity of DG that an active distribution system can safely accommodate. The WDAR-JCC optimization model employs the Wasserstein ambiguity set, a ball in the space of probability distributions centred at the empirical distribution, to hedge against load demand and DG output uncertainties. It also builds upon the distributionally robust approach by empowering it with the adjustable robust counterpart methodology, allowing fast-acting control devices such as inverters to take live recourse actions in response to demand and generation uncertainties. To deal with the uncertain chance constraints, we first define them via the distributionally robust CVaR and then, using tractable convex reformulations, we develop a convex quadratic model. To solve the developed large-scale DG capacity assessment problem, we utilise the ADMM technique. Simulations on the modified IEEE 37-node distribution system show that the proposed approach performs 15% better in terms of total PV installation capacity and PV annual generation compared with the adjustable robust approach. We also show that taking inverters' recourse capabilities into account, unlike the conventional distributionally robust approach, results in up to an increase of 50% in total PV installation capacity and an increase of 40% in PV annual generation.

REFERENCES

[1] E. Mulenga, M. H. Bollen, and N. Etherden, "A review of hosting capacity quantification methods for photovoltaics in low-voltage distribution grids," *International Journal of Electrical Power & Energy Systems*, vol. 115, p. 105445, Feb. 2020.
[2] C. J. Dent, L. F. Ochoa, and G. P. Harrison, "Network distributed gen-

eration capacity analysis using OPF with voltage step constraints," *IEEE Transactions on Power systems*, vol. 25, no. 1, pp. 296-304, Feb. 2010.
[3] S. Abapour, K. Zare, and B. Mohammadi-Ivatloo, "Maximizing penetration level of distributed generations in active distribution networks," in *Proceedings of 2013 Smart Grid Conference (SGC)*, Tehran, Iran, pp. 113-118, Dec. 2013 .
[4] M. Mahmoodi and L. Blackhall, "DER hosting capacity envelope in unbalanced distribution systems," in *Proceedings of 2021 IEEE PES Innovative Smart Grid Technologies Europe (ISGT Europe)*, Espoo, Finland, pp. 1-6, Oct. 2021.
[5] B. Wang, C. Zhang, Z. Y. Dong *et al.*, "Improving hosting capacity of unbalanced distribution networks via robust allocation of battery energy storage systems," *IEEE Transactions on Power Systems*, vol. 36, no. 3, pp. 2174-2185, Oct. 2020.
[6] S. Wang, S. Chen, L. Ge *et al.*, "Distributed generation hosting capacity evaluation for distribution systems considering the robust optimal operation of OLTC and SVC," *IEEE Transactions on Sustainable Energy*, vol. 7, no. 3, pp. 1111-1123, Mar. 2016.
[7] M. Mahmoodi, S. M. Noori, A. Attarha *et al.*, "Impact assessment of active network management schemes on DG capacity of distribution systems," in *Proceedings of 2022 IEEE International Conference on Power Systems Technology (POWERCON)*, Kuala Lumpur, Malaysia, pp. 1-7, Sept. 2022.
[8] P. Dudhe, N. Kadam, R. Hushangabade *et al.*, "Internet of things (IoT): An overview and its applications," in *Proceedings of 2017 International Conference on Energy, Communication, Data Analytics and Soft Computing (ICECDS)*, Chennai, India, pp. 2650-2653, Aug. 2017.
[9] G. Harrison and A. Wallace, "Optimal power flow evaluation of distribution network capacity for the connection of distributed generation," *IEE Proceedings – Generation, Transmission and Distribution*, vol. 152, no. 1, pp. 115-122, Jan. 2005.
[10] L. F. Ochoa, C. J. Dent, and G. P. Harrison, "Distribution network capacity assessment: variable DG and active networks," *IEEE Transactions on Power Systems*, vol. 25, no. 1, pp. 87-95, Nov. 2009.
[11] A. Prékopa, *Stochastic Programming*. Berlin: Springer Science & Business Media, 2013.
[12] D. Bertsimas, D. B. Brown, and C. Caramanis, "Theory and applications of robust optimization," *SIAM review*, vol. 53, no. 3, pp. 464-501, Aug. 2011.
[13] P. M. Esfahani and D. Kuhn, "Data-driven distributionally robust optimization using the Wasserstein metric: performance guarantees and tractable reformulations," *Mathematical Programming*, vol. 171, no. 1, pp. 115-166, Jul. 2017.
[14] G. Calafiore, "Uncertain convex programs: randomized solutions and confidence levels," *Mathematical Programming*, vol. 102, pp. 25-46, Feb. 2004.
[15] S. M. Noori, M. Burgess, M. Mahmoodi *et al*., "An adjustable scenario optimisation approach in operating PV-rich distribution systems," *IEEE Transactions on Power Systems*, vol. 38, no. 5, pp. 4095-4106, Oct. 2022.
[16] M. C. Campi and S. Garatti, "The exact feasibility of randomized solutions of uncertain convex programs," *SIAM Journal on Optimization*, vol. 19, no. 3, pp. 1211-1230, Oct. 2008.
[17] F. Alismail, P. Xiong, and C. Singh, "Optimal wind farm allocation in multi-area power systems using distributionally robust optimization approach," *IEEE Transactions on Power Systems*, vol. 33, no. 1, pp. 536-544, Apr. 2017.
[18] F. Pourahmadi and J. Kazempour, "Distributionally robust generation expansion planning with unimodality and risk constraints," *IEEE Transactions on Power Systems*, vol. 36, no. 5, pp. 4281-4295, Feb. 2021.
[19] S. M. Noori, P. Scott, M. Mahmoodi *et al.*, "Data-driven adjustable robust solution to voltage-regulation problem in PV-rich distribution systems," *International Journal of Electrical Power & Energy Systems*, vol. 141, p. 108118, Oct. 2022.
[20] S. Zymler, D. Kuhn, and B. Rustem, "Distributionally robust joint chance constraints with second-order moment information," *Mathematical Programming*, vol. 137, no. 1, pp. 167-198, Feb. 2013.
[21] A. Ben-Tal, D. den Hertog, A. de Waegenaere *et al*., "Robust solutions of optimization problems affected by uncertain probabilities," *Management Science*, vol. 59, no. 2, pp. 341-357, Nov. 2012.
[22] Y. Zhang, S. Shen, and J. L. Mathieu, "Distributionally robust chance-constrained optimal power flow with uncertain renewables and uncertain reserves provided by loads," *IEEE Transactions on Power Systems*, vol. 32, no. 2, pp. 1378-1388, May 2016.
[23] Z. Wang, Q. Bian, H. Xin *et al.*, "A distributionally robust co-ordinated reserve scheduling model considering cvar-based wind power reserve requirements," *IEEE Transactions on Sustainable Energy*, vol. 7, no. 2, pp. 625-636, Dec. 2015.
[24] X. Chen, W. Wu, B. Zhang *et al.*, "Data-driven DG capacity assessment method for active distribution networks," *IEEE Transactions on Power Systems*, vol. 32, no. 5, pp. 3946-3957, Dec. 2016.
[25] D. Wozabal, "A framework for optimization under ambiguity," *Annals of Operations Research*, vol. 193, no. 1, pp. 21-47, Nov. 2010.
[26] R. Zhu, H. Wei, and X. Bai, "Wasserstein metric based distributionally robust approximate framework for unit commitment," *IEEE Transactions on Power Systems*, vol. 34, no. 4, pp. 2991-3001, Jan. 2019.
[27] C. Duan, W. Fang, L. Jiang *et al.*, "Distributionally robust chance-constrained approximate AC-OPF with Wasserstein metric," *IEEE Transactions on Power Systems*, vol. 33, no. 5, pp. 4924-4936, Feb. 2018.
[28] Y. Guo, K. Baker, E. Dall'Anese *et al*., "Data-based distributionally robust stochastic optimal power flow part I: methodologies," *IEEE Transactions on Power Systems*, vol. 34, no. 2, pp. 1483-1492, Oct. 2018.
[29] V. F. Martins and C. L. Borges, "Active distribution network integrated planning incorporating distributed generation and load response uncertainties," *IEEE Transactions on Power Systems*, vol. 26, no. 4, pp. 2164-2172, Apr. 2011.
[30] A. Ben-Tal, A. Goryashko, E. Guslitzer *et al*., "Adjustable robust solutions of uncertain linear programs," *Mathematical Programming*, vol. 99, no. 2, pp. 351-376, Jan. 2004.
[31] X. Chen, W. Wu, and B. Zhang, "Robust capacity assessment of distributed generation in unbalanced distribution networks incorporating ANM techniques," *IEEE Transactions on Sustainable Energy*, vol. 9, no. 2, pp. 651-663, Sept. 2017.
[32] S. Boyd, N. Parikh, and E. Chu, *Distributed Optimization and Statistical Learning via the Alternating Direction Method of Multipliers*. Boston: Now Publishers, 2011.
[33] C. Wang, R. Gao, F. Qiu *et al.*, "Risk-based distributionally robust optimal power flow with dynamic line rating," *IEEE Transactions on Power Systems*, vol. 33, no. 6, pp. 6074-6086, Jun. 2018.
[34] R. A. Jabr, "Distributionally robust CVaR constraints for power flow optimization," *IEEE Transactions on Power Systems*, vol. 35, no. 5, pp. 3764-3773, Feb. 2020.
[35] W. Wei, F. Liu, and S. Mei, "Distributionally robust co-optimization of energy and reserve dispatch," *IEEE Transactions on Sustainable Energy*, vol. 7, no. 1, pp. 289-300, Nov. 2015.
[36] X. Zhou, M. Farivar, Z. Liu *et al.*, "Reverse and forward engineering of local voltage control in distribution networks," *IEEE Transactions on Automatic Control*, vol. 66, no. 3, pp. 1116-1128, May 2020.
[37] M. Mahmoodi, A. Attarha, S. M. Noori *et al.*, "Adjustable robust approach to increase DG hosting capacity in active distribution systems," *Electric Power Systems Research*, vol. 211, p. 108347, Oct. 2022.
[38] L. R. Araujo, D. Penido, S. Carneiro *et al.*, "A three-phase optimal power-flow algorithm to mitigate voltage unbalance," *IEEE Transactions on Power Delivery*, vol. 28, no. 4, pp. 2394-2402, Sept. 2013.
[39] B. Perera, P. Ciufo, and S. Perera, "Advanced point of common coupling voltage controllers for grid-connected solar photovoltaic (PV) systems," *Renewable Energy*, vol. 86, pp. 1037-1044, Feb. 2016.
[40] B. K. Poolla, A. R. Hota, S. Bolognani *et al.*, "Wasserstein distributionally robust look-ahead economic dispatch," *IEEE Transactions on Power Systems*, vol. 36, no. 3, pp. 2010-2022, Oct. 2020.
[41] R. T. Rockafellar and S. Uryasev, "Optimization of conditional value-at-risk," *Journal of Risk*, vol. 2, pp. 21-42, Jan. 2000.
[42] S. Zhu and M. Fukushima, "Worst-case conditional value-at-risk with application to robust portfolio management," *Operations Research*, vol. 57, no. 5, pp. 1155-1168, Oct. 2009.
[43] S. Boyd and L. Vandenberghe, *Convex Optimization*. Cambridge: Cambridge University Press, 2004, pp. 215-273.
[44] S. Pfenninger and I. Staffell, "Long-term patterns of European PV output using 30 years of validated hourly reanalysis and satellite data," *Energy*, vol. 114, pp. 1251-1265, Nov. 2016.
[45] M. Shaw, B. Sturmberg, L. Guo *et al.*, "The NextGen energy storage trial in the ACT, Australia," in *Proceedings of the Tenth ACM International Conference on Future Energy Systems*, Phoenix, USA, Jun. 2019, pp. 439-442.

Masoume Mahmoodi received the Ph.D. degree in engineering and computer science from The Australian National University (ANU), Canberra, Australia, in 2023. She is a Research Fellow at ANU specialising in distributed energy resources participation optimisation in energy markets. Her research

interests include power system modelling, decision-making under uncertainty, and data-driven power system operation/planning.

Seyyed Mahdi Noori Rahim Abadi received the Bachelors's and Masters's degrees in electrical engineering from Amirkabir University of Technology and the University of Tehran, Tehran, Iran, in 2009 and 2014, respectively. He received the Ph. D. degree in engineering and computer science from The Australian National University (ANU), Canberra, Australia, in 2023. He is currently a Research Fellow at ANU. His research interests include time-series forecasting, power system operation and control, and decision-making under uncertainty.

Ahmad Attarha is a Postdoctoral Fellow at the School of Computing at The Australian National University (ANU), Canberra, Australia. His research interests include intersection of optimisation and power systems, with a specific emphasis on developing distributed optimisation/control techniques that orchestrate distributed energy resources (DERs) to participate in energy and reserve mallet reliably.

Paul Scott received the B.Eng. and B.Sc. degrees from The Australian National University (ANU), Canberra, USA, in 2010, and the Ph.D. degree in computer science from ANU, in 2016. He is currently a Research Fellow in the School of Computing at ANU. His research interests include how optimisation and intelligent systems can enable the integration of DER and renewable energy into electricity systems.

Lachlan Blackhall is an Entrepreneurial Fellow and Head of the Battery Storage and Grid Integration Program at The Australian National University, Canberra, Australia. Previously, he led the development of world-first capabilities to monitor, optimise and control residential solar generation and battery storage as well as the development of virtual power plant technology to aggregate energy storage to deliver services to energy networks, markets and utilities. His research interest includes control of complex systems and networks.